Ubiquity of domain patterns in sheared viscoelastic fluids

E. K. Hobbie,* S. Lin-Gibson, H. Wang,† J. A. Pathak, and H. Kim‡
National Institute of Standards and Technology, Gaithersburg, Maryland 20899, USA
(Received 21 November 2003; published 2 June 2004)

A ubiquitous domain pattern is observed in two-phase viscoelastic fluids falling within the simple paradigm of soft viscoelastic domains suspended in a less viscoelastic fluid under shear flow. Three strikingly different complex fluids exhibit the same shear-induced domain structure, which we relate to the elasticity of the dispersed phase via an approximate Weissenberg number. We suggest a physical mechanism for the formation of this pervasive pattern, independent of the dynamic origin of the elasticity of the suspended phase.

DOI: 10.1103/PhysRevE.69.061503 PACS number(s): 83.50.−v, 82.70.−y, 83.60.Hc

I. INTRODUCTION

Multiphase fluids with well-defined interfaces are encountered in a variety of applications, from plastics engineering and pharmaceuticals to paints, cosmetics, and food products. The use of hydrodynamic forces to process and homogenize these inherently soft materials is also ubiquitous, with simple shear serving as a useful reference point for understanding how the multiphase structure deforms and ruptures in flow. Due to the frequent incorporation of macromolecules within distinct phases, it is common for such fluids to be themselves *viscoelastic*, apart from any interfacial contribution, which has profound implications for processing. Here, we report striking similarities in the domain structure exhibited by three distinct complex fluids under simple shear flow, and we suggest that the pervasive nature of the response stems from a shared coarse-grained scenario of soft viscoelastic domains suspended in a less viscoelastic fluid under shear, with the characteristic features of the pattern arising from flow-mediated interdomain interactions. The critical role of domain elasticity is assessed via an effective Weissenberg number, the magnitude of which suggests that the pattern might be viewed as a collection of weakly interacting localized instabilities.

Two quantities of fundamental interest in the shear response of multiphase fluids are the structure factor $S(\mathbf{q})$ and the two-point correlation function $c(\mathbf{r})$. Both are linked to a binary composition field $\psi(\mathbf{r})$ that maps the presence of heterogeneous droplets or domains. If the dispersed phase is found at position $\mathbf{r}$, then $\psi(\mathbf{r})=1$, with $\psi=0$ otherwise. The correlation function is $c(\mathbf{r})=\langle\psi(\mathbf{r})\psi(0)\rangle$, where the brackets denote an ensemble average, and planar projections of $c(\mathbf{r})$ can be computed from real-space micrographs [1]. The structure factor, which is often measured directly with small-angle light scattering, is the Fourier transform of $c(\mathbf{r})$, or the "power spectrum" of the field $\psi(\mathbf{r})$ in reciprocal space [1]. At any instant and location, the two-phase structure of these fluids is spatially stochastic, but patterns exhibited by $S(\mathbf{q})$ and $c(\mathbf{r})$ reveal statistical trends and correlations.

II. MATERIALS AND METHODS

The first system of interest is a polymer blend with viscoelastic asymmetry between the dispersed and continuous phase, the former being more viscoelastic than the latter [1]. The polymers are polybutadiene (PB) and polyisoprene (PI), with number-averaged molar mass and polydispersity $M_n=51\,000$ and $M_w/M_n=1.04$ for the PB and $M_n=72\,000$ and $M_w/M_n=1.02$ for the PI. The quiescent ratio of domain viscosity to matrix viscosity is 10. The two polymers are immiscible [1], and we focus here on PI volume fractions of 20 % by mass. Mixtures were prepared via solution blending from methylene chloride (the mass fraction of polymer in solution =0.02) containing the appropriate amount of each component and a small amount (mass fraction 5×10^{-4} in solution) of antioxidant. Mixtures were stirred at room temperature for one day and filtered. The solvent was then removed under an atmosphere of flowing nitrogen gas, and the samples were dried in a vacuum oven at room temperature for several days. Measurements were performed at 130° C. The samples were heated from room temperature and annealed for 30 min before shearing to obtain a reproducible initial morphology.

The second system of interest is a physical nanoplatelet-polymer gel in water. The colloidal nanoclay (denoted LRD) is a synthetic hectorite material consisting of 30 nm diameter hydrophilic platelets of 1 nm thickness [2,3]. The polymer is poly(ethylene oxide) (PEO) of molar mass 10^6 g/mol and mean radius-of-gyration [4] (R_g) 70 nm. The sample contains 3 % (mass fraction) clay and 2 % (mass fraction) polymer in distilled, deionized water. The pH is maintained at 10 via the addition of NaOH and the ionic strength is maintained at 10^{-3} mol/L NaCl. The solutions were gently mixed over the course of many weeks and were homogenous and optically transparent prior to shearing, with a slightly opalescent appearance arising from the nanostructure of the clay platelets. In equilibrium, adsorption of PEO segments onto the LRD surface leads to the formation of a physical gel [5,6], with the diffuse polymer chains "bridging" neighboring clay particles, which feel a short-range electrostatic repulsion [2,3,5]. The quiescent or equilibrium phase is miscible in the sense

*Email address: erik.hobbie@nist.gov
†Also at Department of Materials Science and Engineering, Michigan Technological University, Houghton, MI 49931.
‡Also at Department of Chemistry, Kyunghee University, Yongin, Kyungkido 449-701, Korea.

that the samples are macroscopically homogeneous with ideal clay dispersion. The equilibrium structure factor measured with small-angle neutron scattering exhibits a broad isotropic shoulder at $q_0 \approx 0.08\ \mathrm{nm}^{-1}$, corresponding to an equilibrium spacing between platelets of $d = 2\pi/q_0 \approx 80$ nm [6]. All measurements were performed at 25 °C.

The third system of interest is a semidilute carbon nanotube suspension [7]. The multiwalled carbon nanotubes (MWNTs), grown via chemical vapor deposition, have a mean diameter $d \approx 50$ nm (polydispersity ≈ 1.2) and mean length $L \approx 12\ \mu$m (polydispersity ≈ 2.0). The suspending polyisobutylene fluid (PIB, $M_n = 800$, $R_g \approx 1$ nm) is Newtonian over a broad range of shear rates, with a shear viscosity of 10 Pa s at 25 °C, where the measurements described here were performed. Dispersions were prepared by dissolving the PIB in sonicated MWNT-toluene suspensions [7], which were stirred continously as the solvent was removed. The suspensions of interest contain 5×10^{-3} mass-fraction MWNT in PIB and are semidilute, with $nL^3 = (4/\pi)\phi_0(L/d)^2 \approx 125$ and $nL^2 d \approx (4/\pi)\phi_0(L/d) \approx 0.5$ where n is the number of tubes per unit volume and $\phi_0 \approx 1.7 \times 10^{-3}$ is the volume fraction. The nanotubes in PIB are nonsedimenting and non-Brownian, with a Peclet number of order 10^4 or higher [7].

The *in situ* scattering/microscopy instrument is described in detail elsewhere [8]. The flow is along the x axis, with a constant velocity gradient along the y axis and vorticity along the z axis [Fig. 1(a)]. Measurements are taken in the x-z plane, with light-scattering patterns and real-space optical micrographs collected simultaneously. The samples are confined between two parallel quartz plates separated by a variable gap h. The upper plate rotates at an angular speed that sets the shear rate, $\dot{\gamma} = \partial v_x/\partial y$, at a fixed point of observation 2.5 cm from the center of the 4 cm radius plates. Controlled-stress and controlled-strain rheometers in cone-and-plate and parallel-plate configurations were used for steady-shear measurements of the shear viscosity (η), shear shress (σ_{xy}), first normal stress difference ($N_1 = \sigma_{xx} - \sigma_{yy}$), and linear-viscoelastic measurements of the complex shear modulus, $G^*(\omega)$.

III. RESULTS AND DISCUSSION

Figure 1 shows structure observed under shear for (a) the polymer blend at $\dot{\gamma} = 75\ \mathrm{s}^{-1}$, (b) an analogous plot of shear-induced macrostructure in the physical gel at $\dot{\gamma} = 100\ \mathrm{s}^{-1}$, and (c) transient structure exhibited by the semidilute MWNT suspension, where diffuse aggregates form after quenching the initially homogeneous non-Brownian dispersion to $\dot{\gamma} = 0.03\ \mathrm{s}^{-1}$. In all three cases, a similar morphology leads to analogous patterns in $S(\mathbf{q})$ and $c(\mathbf{r})$. The structure in Fig. 1(a) is somewhat distinct from the other two systems in that the quiescent phase is immiscible and thus macroscopically inhomogeneous, whereas the structure in (b) and (c) is shear induced. Additionally, the patern in the MWNT suspension is transient, ultimately giving way to analogous coarser structures as a function of time [7]. Due to the macroscopic size of the MWNT domains, $S(\mathbf{q})$ cannot be measured with light scattering, but is obtained as an FFT of the computed $c(\mathbf{r})$. The three patterns are strikingly similar, and we note that analogous patterns are associated with shear-induced turbidity in semi-dilute polymer solutions [9] and shear-induced clustering in thixotropic clay gels [10], to name just two of a vast number of systems that exhibit this pattern in shear flow.

A common coarse-grained scenario for all three systems would appear to be viscoelastic domains suspended in a less viscoelastic fluid under shear at significant (10–20 %) volume fraction. To further explore and quantify the link between this pattern and the disparate elasticity of the dispersed and continous components, we use steady and oscillatory-shear rheometry. Figure 2 shows steady-shear rheology data for each phase in each of the three scenarios. In Fig. 2(a) the distinction between the two phases is trivial; however, this is not the case in Figs. 2(b) and 2(c), where the domains appear in response to shear and the exact composition is less clear. For the sake of simplicity, we compare the steady-shear response of the physical clay-polymer gel with that of the pure polymer solution to qualitatively assess the viscoelastic asymmetry present in Fig. 1(b). For the nanotube suspension, the domain volume fraction can be computed from optical micrographs, with the domains containing on the order of 3 % MWNT by mass in a suspending fluid of pure PIB [7], and a homogeneous suspension of 3 % MWNT by mass in PIB was thus prepared to mimic the composition of domains in Fig. 1(c). At an approximate internal shear rate $\dot{\gamma}_d = \dot{\gamma}/2$ [11], each of the three systems exhibits emergent elasticity in the dispersed phase, which we quantify in terms of an approximate Weissenberg number [12], $\mathrm{Wi} = N_1/\sigma_{xy}$, evaluated at $\dot{\gamma}_d$ (indicated by a vertical dashed line). We find Wi $\approx 2.5, 4.5$, and 2, for the blend, gel, and suspension, respectively. In contrast, the continous phase in each of the three scenarios is essentially a viscous fluid.

Figure 3 shows small-amplitude oscillatory shear measurements of the complex shear modulus, $G^*(\omega) = G' + iG'' = Ge^{i\delta}$, performed in the linear viscoelastic regime on both the dispersed and continous phase for each of the three binary systems. As before, the two phases in Fig. 3(a) are pure PI and PB, respectively, while in Fig. 3(b) we assume that the gel-like macrodomains have approximately the same composition as the equilibrium gel and reside in a 2 % polymer (PEO) solution. In Fig. 3(c), the continuous phase is again taken to be pure PIB, with diffuse domains containing 3 % MWNT in PIB by mass. The oscillatory shear data further suggest that the dispersed phase in each of the three scenarios is of more or comparable viscoelsticity than the continuous phase. The analog of the Weissenberg number for oscillatory shear is the inverse of the loss tangent, $\cot(\delta) = G'/G''$, which we evaluate at $\omega = \dot{\gamma}_d$ to get 0.50, 4, and 3.5 for the blend, gel, and suspension, respectively. The vertical dashed lines indicate the characteristic angular frequency that we heuristically associate with the applied steady shear rate. This analysis further quantifies the domain elasticity and in each case classifies the suspending fluid as only weakly viscoelastic.

The structure of $c(\mathbf{r})$ is shown in Fig. 4, which plots $c(x_i)$ as a function of x_i/ξ_i for each of the three systems, where the quantity in parentheses is the characteristic length scale used to reduce the horizontal axis. Also shown in (b) is the expo-

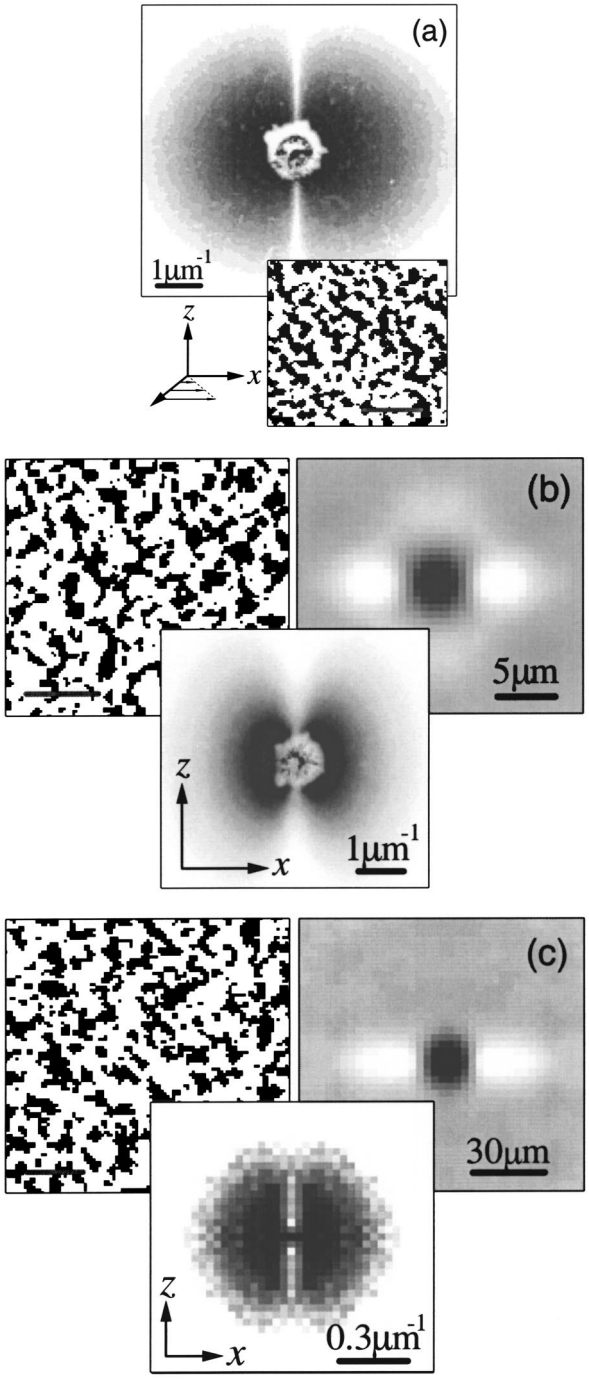

FIG. 1. (a) Light-scattering pattern and binary micrograph (scale bar=20 μm) of an asymmetric polymer blend (PI volume fraction =0.20, T=130° C, $\dot{\gamma}$=75 s^{-1}), with the flow geometry as indicated and a gap of 400 μm (b) Analogous plot of shear-induced macrostructure in a physical colloidal gel (scale bar=20 μm, T =25° C, $\dot{\gamma}$=100 s^{-1}) of 2 % polymer (PEO) and 3 % nanoclay (LRD) in water. The volume fraction of domains is 0.20 and the gap is 450 μm. The pattern is evident in both $c(\mathbf{r})$ (right) and $S(\mathbf{q})$ (lower). (c) Transient structure in a semidilute nanotube suspension (scale bar=60 μm) 15 min after quenching an initially homogeneous dispersion (0.5 % MWNT by mass, T=25 ° C) to $\dot{\gamma}$ =0.03 s^{-1}. The pattern is evident in $c(\mathbf{r})$ and its FFT, $S(\mathbf{q})$ (lower). The volume fraction of domains is approximately 0.2 and the gap is 50 μm.

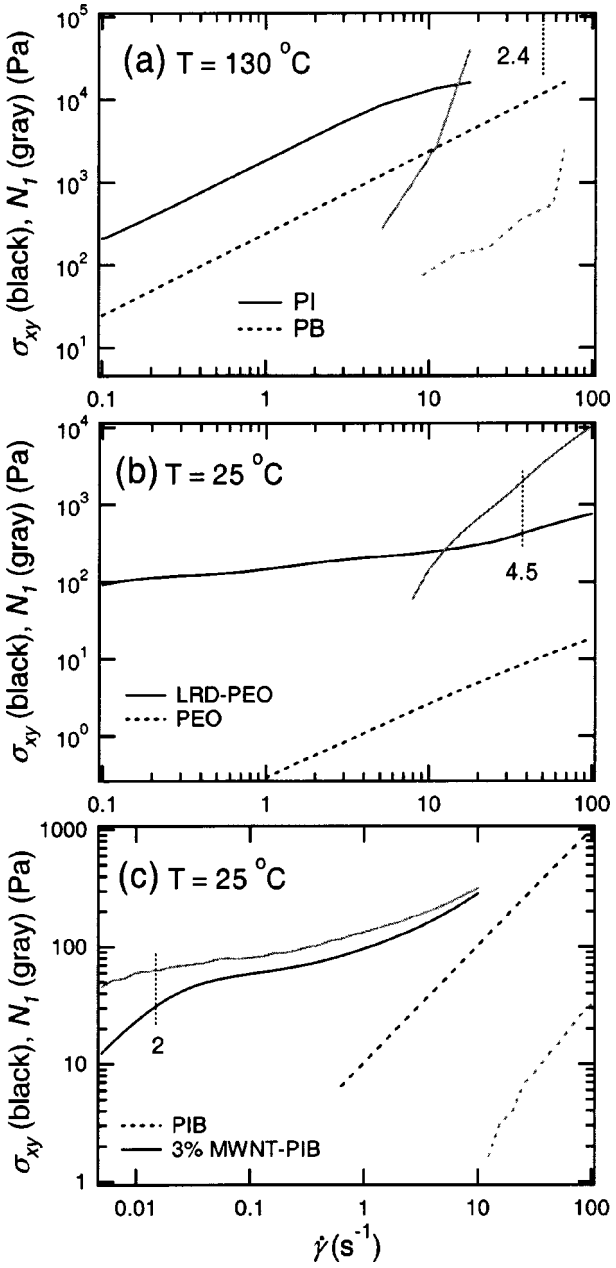

FIG. 2. Steady-shear response of the dispersed and continuous phase for the three fluids depicted in Fig. 1, where the vertical dashed lines indicate the approximate shear rate inside a domain, $\dot{\gamma}_d \approx \dot{\gamma}/2$. An approximate Weissenberg number (Wi) for the droplet phase, defined as the ratio of N_1 to σ_{xy} evaluated at $\dot{\gamma}_d$, is indicated in each case. In (a), values at the highest shear rate measured are used to estimate Wi.

nential decay $c(x_i)=\exp(-2x_i/\xi_i)$, which we use in the $x_i \rightarrow 0$ limit to extract the correlation lengths ξ_x and ξ_z [1]. Although the presence of correlation minima in $c(\mathbf{r})$ implies that the structure is *not* random along $\hat{\mathbf{x}}$, interactions are less important in the limit of small displacements, and this analysis gives a consistent measure of size, shape, and position in the *x*-*z* plane. The structure shown in Fig. 4(a), with a weak minimum along the *x* axis, is universal to the pattern in question, which has correlation minima symmetrically positioned along the flow direction in the *x*-*z* plane. In all three of these

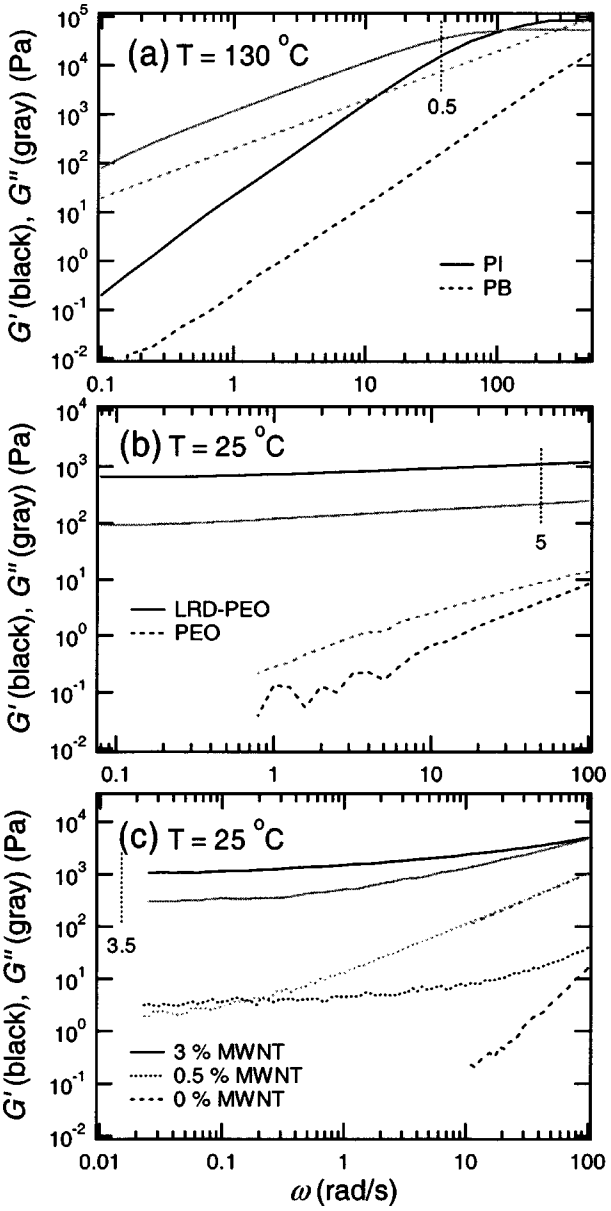

FIG. 3. Linear-viscoelastic response of the dispersed and continous phase for the three fluids depicted in Fig. 1, where the vertical dashed lines indicate the characteristic frequency that we qualitatively associate with the applied shear rate. In each case, the inverse loss tangent (defined as the ratio of storage to loss modulus) evaluated at the characteristic frequency $\omega = \dot{\gamma}/2$ is indicated.

systems, the correlation lengths reflect the mean domain size, which is dictated by a balance of flow-induced viscous and elastic forces, which will tend to rupture the domains, and the effects of surface tension, bond strength, and friction, which will tend to hold the domains together.

IV. CONCLUSIONS

Tanaka [13] has suggested that binary fluids with viscoelastic asymmetry fall into a distinct class of phase-ordering kinetics. Our results suggest that the same might be true of the morphology of such fluids in response to shear

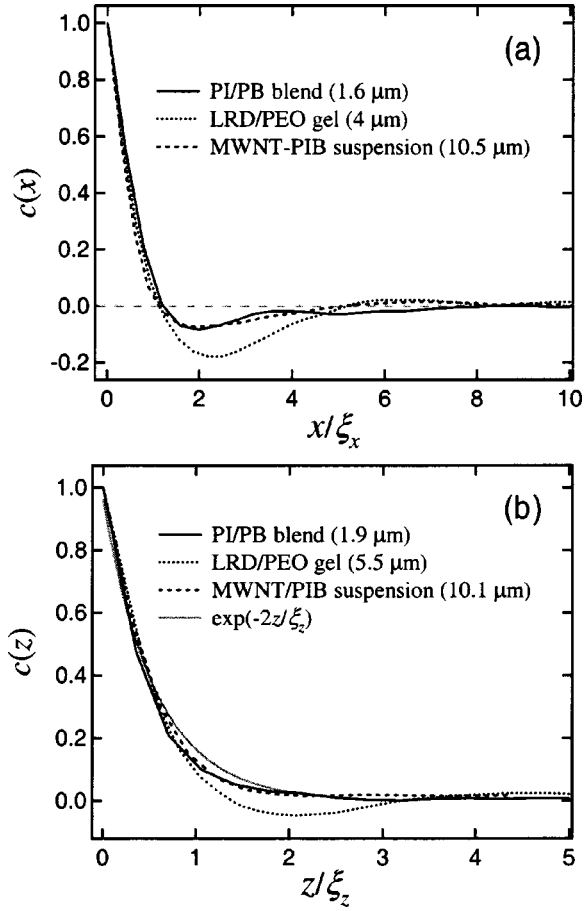

FIG. 4. (a) $c(x)$ as a function of x/ξ_x and (b) $c(z)$ as a function of z/ξ_z for the three systems depicted in Fig. 1, where the quantity in parentheses is the measured characteristic length scale used to reduce the horizontal axis.

flow. The origin of this structure is intriguing and warrants further consideration, but heuristically, we suggest that it might arise from the unstable nature of the domains. For an isolated viscoelastic droplet in shear flow, it has been demonstrated that internal elastic forces related to the first normal stress difference N_1 lead to droplet elongation along the vorticity axis, while the "orbits" of such isolated droplets are inherently unstable, showing irregular "rocking" motion somewhat reminiscent of the periodic orbits exhibited by rigid rods [1,14]. A suspension of such droplets would exhibit this same tendency, albeit with a much more complicated flow field. We suggest that "crowding" of these orbits along the direction of flow might give rise to interaction effects, evident as correlation minimum in $c(\mathbf{r})$ and lobes of strong scattering in $S(\mathbf{q})$. As this tendency emerges with increasing Wi, it falls within the broader context of "elastic turbulence" [15], with the instability occurring on a localized scale and interactions giving rise to the characteristic pattern. A detailed analysis of the three systems considered here suggests a critical Weissenberg number of around 0.5. We conclude by noting that any system with weak periodicity and weak elongation along two sets of perpendicular axes will exhibit this same pattern, which itself is much broader than the specific context of interest here.

[1] E. K. Hobbie *et al.*, J. Chem. Phys. **117**, 6350 (2002).
[2] M. Kroon, W. L. Vos, and G. H. Wegdam, Phys. Rev. E **57**, 1962 (1998).
[3] J. D. Ramsay, S. W. Swanton, and J. Bunce, J. Chem. Soc., Faraday Trans. **86**, 3919 (1990).
[4] K. Devanand and J. C. Selser, Macromolecules **24**, 5943 (1991).
[5] J. Swenson, M. V. Smalley, H. L. M. Hatharasinghe, and G. Fragneto, Langmuir **17**, 3813 (2001).
[6] G. Schmidt *et al.*, Macromolecules **33**, 7219 (2000); **35**, 4725 (2002); S. Lin-Gibson *et al.*, J. Chem. Phys. **119**, 8080 (2003).
[7] S. Lin-Gibson *et al.*, Phys. Rev. Lett. **92**, 048302 (2004).
[8] S. Kim *et al.*, Rev. Sci. Instrum. **67**, 3940 (1996).
[9] E. Moses, T. Kume, and T. Hashimoto, Phys. Rev. Lett. **72**, 2037 (1994).
[10] F. Pignon, A. Magnin, and J.-M. Piau, Phys. Rev. Lett. **79**, 4689 (1997).
[11] Simple shear flow contains equal parts pure elongation (directed along $y=x$ at a rate of $\dot{\gamma}/2$) and pure rotation (about $\hat{\mathbf{z}}$ at a rate of $\dot{\gamma}/2$). For a droplet with nearly spherical symmetry, the effective internal rate of strain is thus approximately half the applied shear rate. Although the domains encountered here are not spherical, the ensemble-averaged aspect ratio is not far removed from unity, and we adopt this convention as a first approximation.
[12] See, for example, R. B. Bird, R. C. Armstrong, and O. Hassager, *Dynamics of Polymeric Liquids* (Wiley, New York, 1987), Vol. 1.
[13] H. Tanaka, Phys. Rev. Lett. **76**, 787 (1996); H. Tanaka and T. Araki, *ibid.* **79**, 4966 (1997).
[14] E. K. Hobbie and K. B. Migler, Phys. Rev. Lett. **82**, 5393 (1999); F. Mighri and M. A. Hureault, J. Rheol. **45**, 783 (2001).
[15] R. G. Larson, Nature (London) **405**, 27 (2000).